Automated Generation of Geometric Models for a Bulbous Trawler Ship

Louis Blanchard, Régis Duvigneau, Bernard Mourrain

Automated Generation of Geometric Models for a Bulbous Trawler Ship

Louis Blanchard, Régis Duvigneau, Bernard Mourrain

RESEARCH REPORT
N° 8011
July 2012
Project-Teams Opale and Galaad

ISSN 0249-6399   ISRN INRIA/RR--8011--FR+ENG

Automated Generation of Geometric Models for a Bulbous Trawler Ship

Louis Blanchard*, Régis Duvigneau*, Bernard Mourrain†

Project-Teams Opale and Galaad

Research Report n° 8011 — July 2012 — 16 pages

Abstract: The objective of this work is to develop an automated geometric modeler for trawler ships including a bow, for shape optimization purpose. Two approaches are tested to generate a spline-based representation of the hull. For the first one, a starting shape without bow is deformed to reach a target composed of points or lines, while preserving the shape regularity using a penalty functional. For the second approach, a starting hull including a baseline bow is deformed by handling meta-parameters, such as bow length, thickness or orientation. The different approaches are finally illustrated for a realistic application.

Key-words: parameterization, shape, bow, splines

* Opale Project-Team
† Galaad Project-Team

RESEARCH CENTRE
SOPHIA ANTIPOLIS – MÉDITERRANÉE

2004 route des Lucioles - BP 93
06902 Sophia Antipolis Cedex

Génération automatique de modèles géométriques pour un chalutier avec bulbe

Résumé : L'objectif de ce travail est de développer un modeleur géométrique automatique pour les chalutiers avec bulbe d'étrave, dans le but de réaliser une optimisation de forme. Deux approches sont testées pour générer une représentation spline de la carène. Dans le premier cas, une forme initial sans bulbe est déformée de manière à atteindre une cible composée de lignes ou de points, tandis que la régularité de la forme est préservée en utilisant une fonctionnelle de pénalisation. Dans le second cas, une carène initiale incluant une forme basique de bulbe est déformée par manipulation de méta-paramètres, comme la longueur, l'épaisseur ou l'orientation du bulbe. Les différentes approches sont finalement illustrées pour une application réelle.

Mots-clés : paramétrisation, forme, bulbe, splines

1 Introduction

Numerical simulations associated with automated design optimization tools can now be used for practical problems in naval hydrodynamics, thanks to the robustness of simulation methods and the increase of computational facilities. A major difficulty in this context is the automated generation of geometric models, defined by a few design parameters, and the corresponding computational grid.

Therefore, we study in this work how to generate automatically a parameterized hull shape model, including a bow, with application to trawler ships. The final objective is to include the developed tool into a design optimization procedure, that allows to automatically optimize the bow shape.

The primary objective of the geometrical model is to facilitate the modification of an existing hull shape by modifying a small number of parameters, that are meaningful for naval architects (see figure 1).

Two approaches are considered successively: for the first one, a starting shape without bow is deformed to reach a target composed of points or lines, while preserving the shape regularity using a penalty functional. For the second approach, a starting hull including a baseline bow is deformed by handling meta-parameters, such as bow length, thickness or orientation.

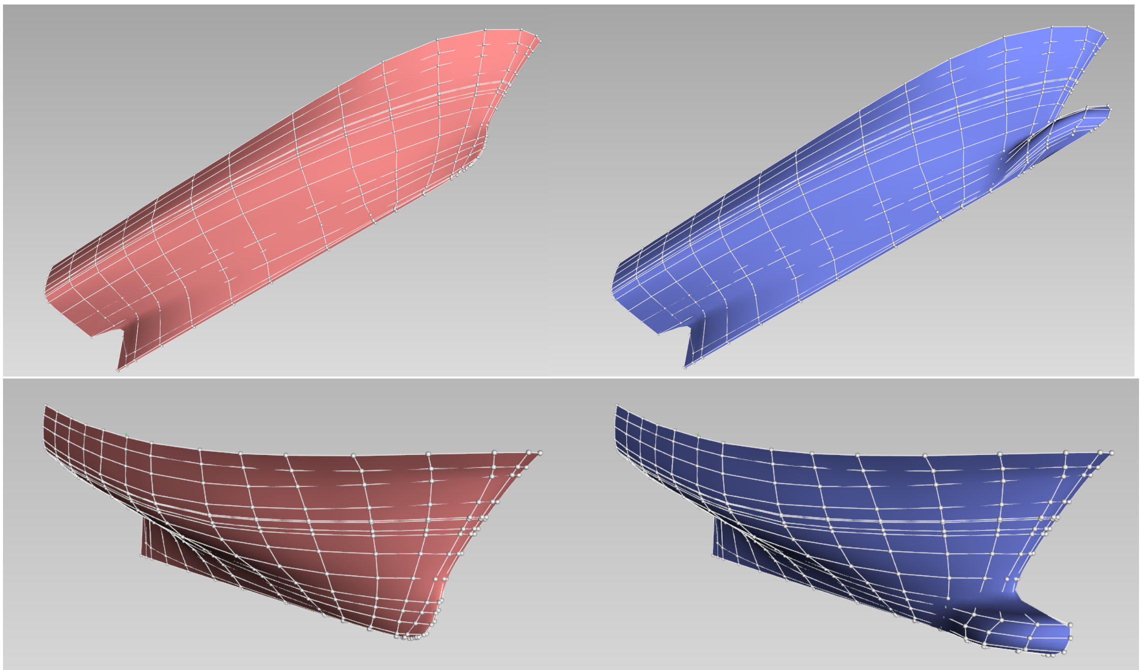

Figure 1: Initial shape (left) and deformed shape to generate a bow (right) for a trawler ship.

2 Fitting approach

2.1 Distance error minimization

We propose first to generate bow shapes from an existing hull without bow. The method consists in fitting the hull surface to a target bow defined by point clouds, by distance minimization.

We refer to articles [1], [4] and [6] for a detailed review of distance minimization problems. Three methods are commonly used to approximate a target shape defined by a set of points cloud: the point distance minimisation (PDM), tangent distance minimisation (TDM) and Squared Distance minimization (SDM). See article [6] and the internship report [5] for a comparison of these methods.

2.1.1 Definition of distance error term

We denote $\otimes$ the tensorial product. Let us consider for $\xi \in \mathbb{R}^3$ the B-spline surface:

$$\sigma_c(\xi) \overset{def}{=} \big(Id_3 \otimes B^T(\xi)\big)\, c \tag{1}$$

where $B(\xi) \in \mathbb{R}^n$ is the vector of B-spline basis functions and $c \in \mathbb{R}^{3n}$ is the vector of control points. We consider the following problem: for a given bow shape, defined by a set of data points X_k , $\forall k \in [1, M]$, compute the B-spline surface to approximate the points X_k.

For a fixed $k \in [1, M]$ we denote $\sigma_c(\xi_k)$ the point of the surface $\sigma_c(\xi)$ that minimizes the distance between the point X_k and the surface $\sigma_c(\xi)$: $d\big(\sigma_c(\xi_k), X_k\big) = argmin \|\, \sigma_c(\xi) - X_k \,\|_{\mathbb{R}^3}$. Using the following notations : $B_k \overset{def}{=} B(\xi_k)$, $A_k \overset{def}{=} Id_3 \otimes B_k^T$ we get:

$$\sigma_c(\xi_k) = \big(Id_3 \otimes B_k^T\big)c = A_k\, c \tag{2}$$

We defined the **Point Distance minimization (PDM)** function as follows :

$$\boxed{e_k(c) = \frac{1}{2} \,\|\, \sigma_c(\xi_k) - X_k \,\|^2_{\mathbb{R}^3}} \tag{3}$$

We defined the **Tangente Distance minimization (TDM)** function as follows :

$$\boxed{\tilde{e}_k(c) = \frac{1}{2}\big(\langle \sigma_c(\xi_k) - X_k \,,\, N_k \rangle_{\mathbb{R}^3}\big)^2} \tag{4}$$

where N_k is the external normal vector of the point $\sigma_c(\xi_k)$.

Finally, we defined **the Squared Distance minimization (SDM)** function as follows :

$$\boxed{\bar{e}_k(c) = \tilde{e}_k(c) + \frac{1}{2}\begin{cases} \frac{d_k}{d_k+\rho_k^u}\big(\langle \sigma_c(\xi_k) - X_k \,,\, T_k^u \rangle_{\mathbb{R}^3}\big)^2 + \frac{d_k}{d_k+\rho_k^v}\big(\langle \sigma_c(\xi_k) - X_k \,,\, T_k^v \rangle_{\mathbb{R}^3}\big)^2 & \text{if } d_k > \max(\rho_k^u, \rho_k^v) \\ 0 & \text{otherwise} \end{cases}} \tag{5}$$

where T_k^u and T_k^v are the tangential vectors of the point $\sigma_c(\xi_k)$, (ρ_k^u, ρ_k^v) are the curvatures of the point $\sigma_c(\xi_k)$ and where $d_k = e_k(c) = \|\, \sigma_c(\xi_k) - X_k \,\|^2_{\mathbb{R}^3}$ is supposed to be fixed on c.

2.1.2 Minimization

In this section we consider the minimization of the distance error term. The problem can be seen as the non linear problem:

$$J(c) = \sum_{k=1}^{M} e_k(c) \quad , \quad \tilde{J}(c) = \sum_{k=1}^{M} \tilde{e}_k(c) \quad , \quad \bar{J}(c) = \sum_{k=1}^{M} \bar{e}_k(c) \tag{6}$$

To solve these problems, we consider deterministic descent methods, based on the computation of gradient and of Hessian of the cost function. The iterative method consists in computing the update $c_{t+1} = c_t + \alpha_t \, d_t$, where $d_t \in \mathbb{R}^n$ is a descent direction and $\alpha_t \in \mathbb{R}^+$ is a step length obtained by a line search :

$$\alpha_t = \arg \min_{\alpha \in \mathbb{R}^+} \; J(c_t + \alpha \, d_t) \tag{7}$$

We refer to the book [2] for a detailed review of deterministic optimization methods. Here, we simply consider the following methods :

- **gradient method** : with the following update for the descent direction :

$$\forall t \in \mathbb{N}^* \quad , \quad d_t \; = \; -\nabla J(c_t) \tag{8}$$

- **Newton-Raphson method** : where the descent direction is the solution of the linear system :

$$\forall t \in \mathbb{N} \quad , \quad \nabla^2 J(c_t) \; d_t \; = \; -\nabla J(c_t) \tag{9}$$

The next propositions allow to evaluate the derivatives of cost functions defined by Eq(6).

Proposition: The fist and second derivatives of the cost function Eq(6) based on the Point Distance minimization function Eq(3) are :

$$\boxed{\begin{array}{l} \nabla J(c) = \displaystyle\sum_{k=1}^{M} \nabla e_k(c) \quad \text{where} \quad \nabla \, e_k(c) \; = \; \big(\sigma_c(\xi_k) - X_k\big) \otimes B_k \\ \nabla^2 J(c) = \displaystyle\sum_{k=1}^{M} \nabla^2 e_k(c) \quad \text{where} \quad \nabla^2 \, e_k(c) \; = \; \big(Id_3 \otimes B_k \, B_k^T\big) \end{array}} \tag{10}$$

Proof: Using the definition of Point Distance minimization function from Eq(3), we get

$$e_k(c) = \frac{1}{2} \langle A_k \, c - X_k \, , \, A_k \, c - X_k \rangle_{\mathbb{R}^3} = \frac{1}{2} \big[\langle c \, , \, A_k^T \, A_k \, c \rangle_{\mathbb{R}^{3n}} - 2 \, \langle c \, , \, A_k^T \, X_k \rangle_{\mathbb{R}^{3n}} + \| \, X_k \, \|_{\mathbb{R}^3}^2 \big]$$

Consequently, the gradient of the Point Distance minimization function turns into :

$$\begin{aligned} \nabla \, e_k(c) &= A_k^T \, A_k \, c - A_k^T \, X_k = \big(Id_3 \otimes B_k\big)\big(Id_3 \otimes B_k^T\big) \, c - \big(Id_3 \otimes B_k\big) \, X_k \\ &= \big(Id_3 \otimes B_k \, B_k^T\big) \, c - \big(Id_3 \otimes B_k\big) \, X_k \\ &= \big(Id_3 \otimes B_k\big)\sigma_c(\xi_k) - \big(Id_3 \otimes B_k\big) \, X_k = \big(\sigma_c(\xi_k) - X_k\big) \otimes B_k \end{aligned}$$

and the Hessian of the Point Distance minimization function turns into :

$$\nabla^2 \, e_k(c) \; = \; A_k^T \, A_k \; = \; \big(Id_3 \otimes B_k\big)\big(Id_3 \otimes B_k^T\big) \; = \; \big(Id_3 \otimes B_k \, B_k^T\big)$$

Proposition: The fist and second derivatives of the cost function Eq(6) based on the Tangente Distance minimization function Eq(4) are :

$$\boxed{\begin{array}{l} \nabla \tilde{J}(c) = \displaystyle\sum_{k=1}^{M} \nabla \tilde{e}_k(c) \quad \text{where} \quad \nabla\, \tilde{e}_k(c) \;=\; \langle \sigma_c(\xi_k) - X_k \,,\, N_k \rangle_{\mathbb{R}^3}\, N_k \otimes B_k \\ \nabla^2 \tilde{J}(c) = \displaystyle\sum_{k=1}^{M} \nabla^2 \tilde{e}_k(c) \quad \text{where} \quad \nabla^2\, \tilde{e}_k(c) \;=\; \big(N_k\, N_k^T \otimes B_k\, B_k^T\big) \end{array}} \tag{11}$$

Proof: Using the definition of the Tangente Distance minimization function from Eq(4), we get

$$\tilde{e}_k(c) = \frac{1}{2}\big(\langle c \,,\, A_k^T\, N_k \rangle_{\mathbb{R}^{3n}} - \langle X_k \,,\, N_k \rangle_{\mathbb{R}^3}\big)^2$$

Consequently, the gradient of the Tangente Distance minimization function turns into :

$$\begin{aligned} \nabla\, \tilde{e}_k(c) &= \langle \sigma_c(\xi_k) - X_k \,,\, N_k \rangle_{\mathbb{R}^3}\, A_k^T\, N_k = \langle \sigma_c(\xi_k) - X_k \,,\, N_k \rangle_{\mathbb{R}^3} \big(Id_3 \otimes B_k\big)\, N_k \\ &= \langle \sigma_c(\xi_k) - X_k \,,\, N_k \rangle_{\mathbb{R}^3}\, N_k \otimes B_k \end{aligned}$$

and the Hessian of the Tangente Distance minimization function turns into :

$$\begin{aligned} \nabla^2\, \tilde{e}_k(c) \;&=\; (A_k^T\, N_k)\,(A_k^T\, N_k)^T \;=\; A_k^T\, N_k\, N_k^T\, A_k = \big(Id_3 \otimes B_k\big)\, N_k\, N_k^T \big(Id_3 \otimes B_k^T\big) \\ &=\; \big(N_k \otimes B_k\big)\big(N_k^T \otimes B_k^T\big) \;=\; \big(N_k\, N_k^T \otimes B_k\, B_k^T\big) \end{aligned}$$

Proposition: The fist and second derivatives of the cost function Eq(6) based on the Squared Distance minimization function Eq(5) are :

$$\boxed{\nabla \bar{J}(c) = \sum_{k=1}^{M} \nabla \bar{e}_k(c) \quad , \quad \nabla^2 \bar{J}(c) = \sum_{k=1}^{M} \nabla^2 \bar{e}_k(c)} \tag{12}$$

where

$$\boxed{\nabla\, \bar{e}_k(c) \;=\; \nabla\, \tilde{e}_k(c) + \left\{ \begin{array}{l} \Big[\frac{d_k}{d_k+\rho_k^u} \langle \sigma_c(\xi_k) - X_k \,,\, T_k^u \rangle_{\mathbb{R}^3}\, T_k^u + \frac{d_k}{d_k+\rho_k^v} \langle \sigma_c(\xi_k) - X_k \,,\, T_k^v \rangle_{\mathbb{R}^3}\, T_k^v\Big] \otimes B_k \\ 0 \end{array} \right.} \tag{13}$$

$$\boxed{\nabla^2\, \bar{e}_k(c) \;=\; \nabla^2\, \tilde{e}_k(c) + \left\{ \begin{array}{ll} \frac{d_k}{d_k+\rho_k^u}\, T_k^u\, \big[T_k^u\big]^T + \frac{d_k}{d_k+\rho_k^v}\, T_k^v\, \big[T_k^v\big]^T & \text{if } d_k > \max(\rho_k^u, \rho_k^v) \\ 0 & \text{otherwise} \end{array} \right.} \tag{14}$$

Proof: Using that d_k is supposed to be fixed on $\mathbf{c}$, and proposition Eq(10)

2.1.3 Numerical experiments

We present in this section the results obtained using the Newton-Raphson method from equation Eq(9). The cost function considered is $\bar{J}(c)$ defined by Eq(6). The initial hull shape, without bow, originates from the test-case defined in the national project BULBE (see acknowledgement section). The bow shape, defined by point clouds X_k $\forall k \in [1, M]$ is represented by two line targets (in red on figure 2). Figure 2 represents, initial shapes of the trawler ship (on the left) and optimal shapes of the trawler ship (on the right).

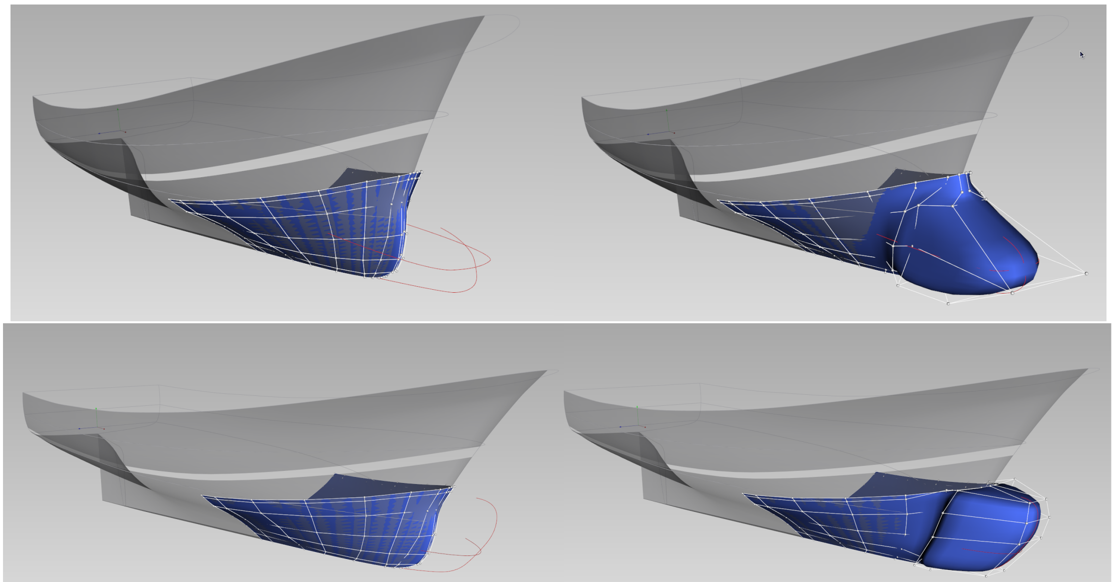

Figure 2: Initial shape (left) and deformed shape to generate a bow (right) for the trawler ship, to reach two line targets (in red).

These tests illustrate the efficiency of the Distance error term minimization approach applied to a trawler ship for generating bows (see figure 2). However, we have observed that this approach suffers from serious drawbacks: the method does not care about the smoothness of the resulting shapes. In practice, the bow shapes obtained exhibit irregularities that are not suitable for industrial use. To overcome this difficulty, we propose to introduce a penalty term that will regularize the problem and ensure a smooth solution surface.

2.2 Smoothness measure minimization

2.2.1 Definition of smoothness measure term

The smoothness measure term of a B-spline surface $S = \sigma_c(\xi)$ is the space integral over the B-spline surface S of the first order derivatives of the mapping function:

$$\boxed{J_s(c) = \int_{\sigma_c(\xi)} tr\big(D\sigma_c(\xi)[D\sigma_c(\xi)]^T\big)\, d\Omega = \int_{\sigma_c(\xi)} \big(\, \| \, \partial_u \sigma_c(\xi) \, \|^2_{\mathbb{R}^3} + \| \, \partial_v \sigma_c(\xi) \, \|^2_{\mathbb{R}^3} \,\big)\, d\Omega} \tag{15}$$

2.2.2 Optimization of smoothness measure term

Proposition: The derivatives of smoothness measure from Eq(15) are:

$$\boxed{\begin{aligned} \nabla\, J_s(c) \;&=\; \int_S \big[\partial_u\sigma_c(\xi) \otimes B_u(\xi) + \partial_v\sigma_c(\xi) \otimes B_v(\xi)\big]\, d\Omega \\ \nabla^2\, J_s(c) \;&=\; Id_3 \otimes \int_S \Big[B_u(\xi)[B_u(\xi)]^T + B_v(\xi)[B_v(\xi)]^T\Big]\, d\Omega \end{aligned}} \tag{16}$$

where :

$$B_u(\xi) = \partial_u B(\xi) \quad , \quad B_v(\xi) = \partial_v B(\xi) \tag{17}$$

Proof: Using equations Eq(1), Eq(17) and the following noation $A_u(\xi) = \partial_u A(\xi)$ and $A_v(\xi) = \partial_v A(\xi)$, we get

$$\begin{aligned} \partial_u\sigma_c(\xi) &= \big(Id_3 \otimes [B_u(\xi)]^T\big)c = A_u(\xi)\, c \\ \partial_v\sigma_c(\xi) &= \big(Id_3 \otimes [B_v(\xi)]^T\big)c = A_v(\xi)\, c \end{aligned} \tag{18}$$

Consequently the definition of the smoothness measure from Eq(15) becomes:

$$\begin{aligned} J_s(c) =& \int_S \Big[\langle c\,,\, [A_u(\xi)]^T\, A_u(\xi)\, c\rangle_{\mathbb{R}^{3n}} + \langle c\,,\, [A_v(\xi)]^T\, A_v(\xi)\, c\rangle_{\mathbb{R}^{3n}}\Big]\, d\Omega \\ =&\langle c\,,\, \Big[\int_S [A_u(\xi)]^T\, A_u(\xi) + [A_v(\xi)]^T\, A_v(\xi)\, d\Omega\Big]\, c\rangle_{\mathbb{R}^{3n}} \end{aligned}$$

Consequently, the gradient of the smoothness measure from Eq(15) turns into :

$$\begin{aligned} \nabla\, J_s(c) &= \Big[\int_S [A_u(\xi)]^T\, A_u(\xi) + [A_v(\xi)]^T\, A_v(\xi)\, d\Omega\Big]\, c \;=\; \int_S \Big[[A_u(\xi)]^T\, \partial_u\sigma_c(\xi) + [A_v(\xi)]^T\, \partial_v\sigma_c(\xi)\Big]\, d\Omega \\ &= \int_S \Big[\big(Id_3 \otimes B_u(\xi)\big)\, \partial_u\sigma_c(\xi) + \big(Id_3 \otimes B_v(\xi)\big)\, \partial_v\sigma_c(\xi)\Big]\, d\Omega \\ &= \int_S \Big[\partial_u\sigma_c(\xi) \otimes B_u(\xi) + \partial_v\sigma_c(\xi) \otimes B_v(\xi)\Big]\, d\Omega \end{aligned}$$

and the hessian of the smoothness measure from Eq(15) turns into :

$$\begin{aligned} \nabla^2\, J_s(c) &= \int_S \Big[[A_u(\xi)]^T\, A_u(\xi) + [A_v(\xi)]^T\, A_v(\xi)\Big]\, d\Omega \;=\; \int_S \Big[Id_3 \otimes \big(B_u(\xi)[B_u(\xi)]^T + B_v(\xi)[B_v(\xi)]^T\big)\Big]\, d\Omega \\ &= Id_3 \otimes \int_S \Big[B_u(\xi)[B_u(\xi)]^T + B_v(\xi)[B_v(\xi)]^T\Big]\, d\Omega \end{aligned}$$

2.2.3 Numerical experiments

This section presents some numerical experiments using an abstract three dimensional surface, to demonstrate the efficiency of the Newton-Raphson optimization method, applied to the reduction of the smoothness measure term J_s from equation Eq(16). The initial shape exhibits very large irregularities, that we would like to reduce. It is represented in blue on figure 3 and is composed of 20^2 control points. The boundaries points define a square and are supposed to be fixed during the optimization process. Consequently the number of control points to be optimized is 18^2 (in three dimension). Consequently the size of the optimization problem is 972. The figure 3 illstrates the evolution of the surface, for different iterations of the optimization process. The figure 4 presents the evolution of the cost function J_s (in blue) and the norm of the cost function $|\nabla J_s|$ (in red) during the optimization process.

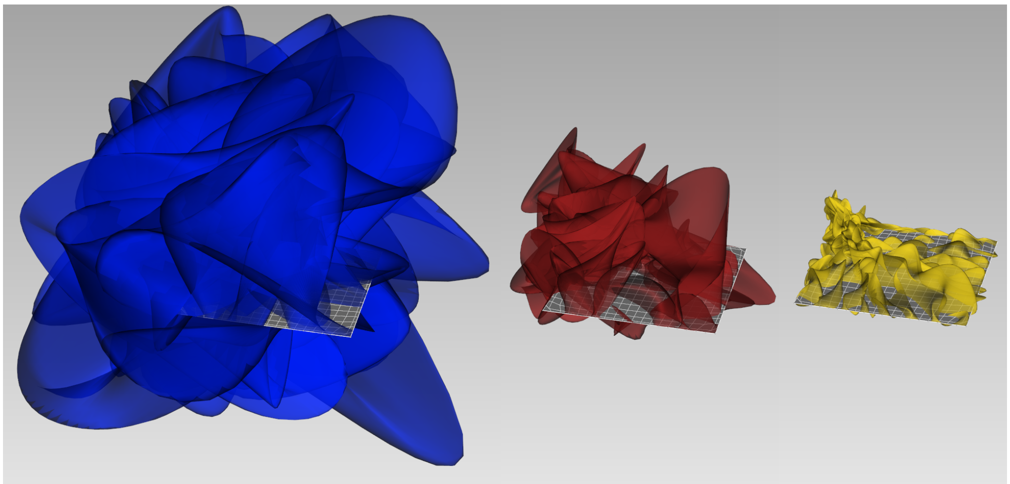

Figure 3: Initial shape (blue) shape after 400 iterations (red), shape after 600 iterations (yellow) and optimal shape (grey).

We obtain promising results for the Smoothness measure term minimization approach applied to a three dimensional surface test-case (see figures 3 and 4).

However, for the initial problem which consists in generating a bow shape, we have to consider an objective function that combines both the Distance error term and the Smoothness mesure term:

$$\boxed{\bar{J}(c) + \lambda\, J_s(c)} \tag{19}$$

where λ is a positive coefficient used to modulate the weight of J_s. It has been found in practical tests with the trawler ship that the results depend strongly on the penalty coefficient and the application of this approach is tedious for industrial cases.

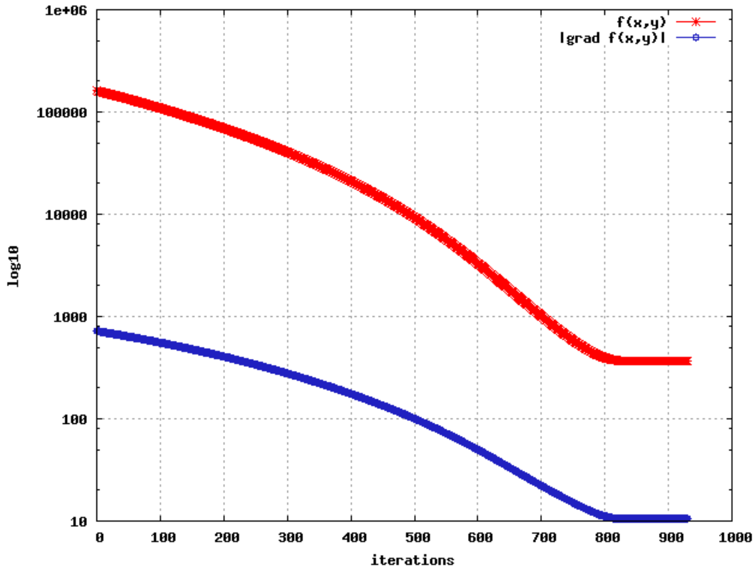

Figure 4: Evolution of the cost function during the optimization process.

3 Direct manipulation of meta-parameters

In this section we propose to generate bow shapes by modifying some meta-parameters, such as width, length or leading direction, from a baseline bow shape.

Using the geometrical model of the trawler ship without bow, we extract a sub-surface that would correspond to the location of a bow surface (see figure 5 on the left). Then, we generate a baseline bow surface by moving the control points of this sub-surface (see figure 5 on the right). The whole geometrical model (hull+bow) can finally be obtained by reconnecting the two surfaces.

The geometrical characteristics of the bow can be controlled by modifying some meta-parameters, such as width, length or leading direction. Each modification of a parameter value is applied to the control points that define the bow surface, as a global transformation. Figure 6 presents some different bow shapes obtained by modifications of width and thickness parameters.

Obviously, this approach is far easier to use than the previous one, but it is more limited in terms of resulting shapes.

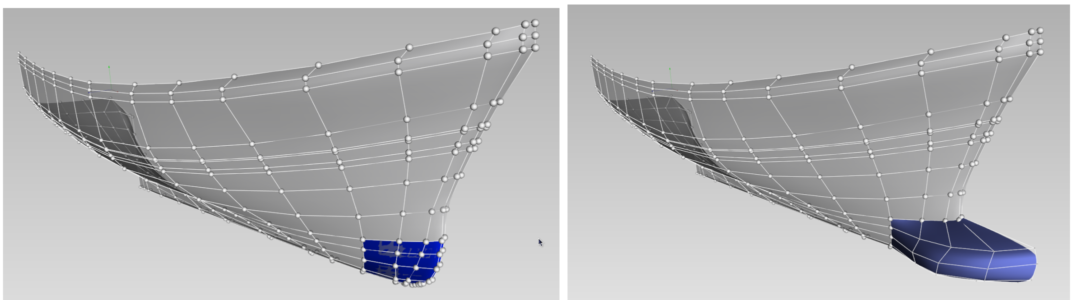

Figure 5: Initial shape (left) and deformed shape to generate a bow (right) for the trawler ship.

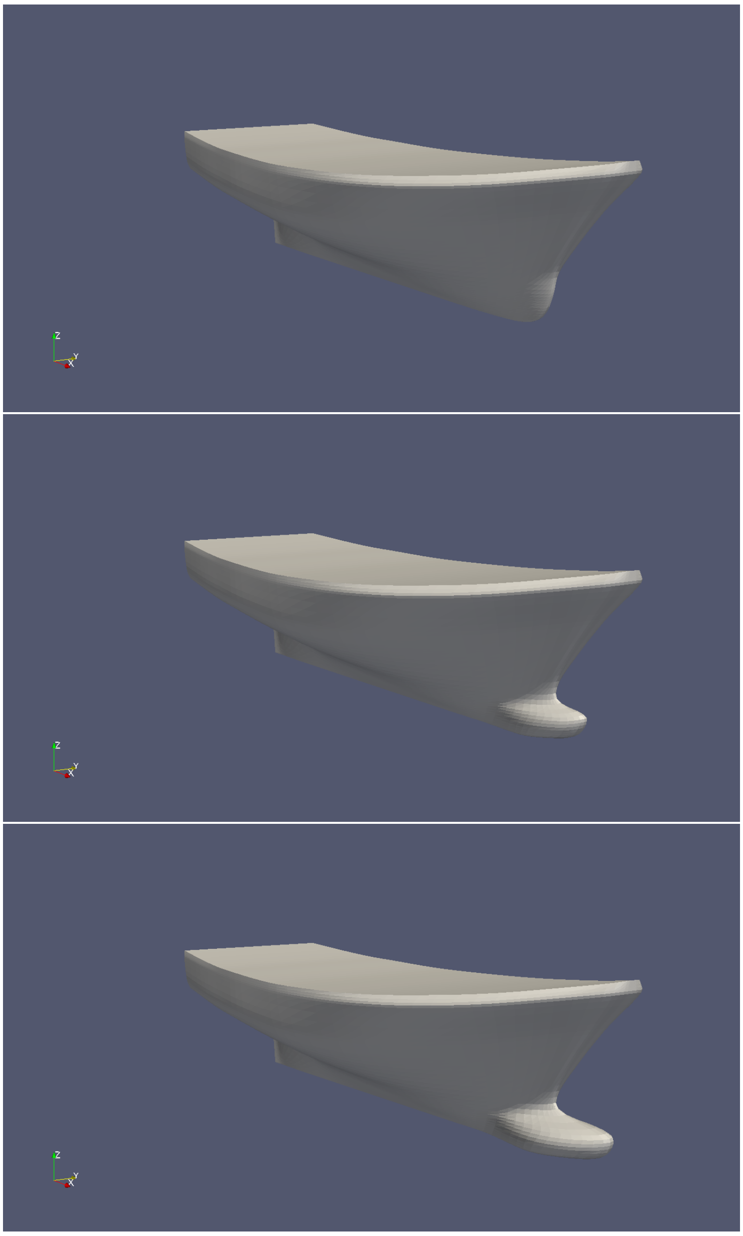

Figure 6: Initial shape (top), deformed shapes : length = 1.5 width = 0.5 (middle), length = 2.5 width = 0.8 (bottom) .

4 Software framework for design optimization

For design optimization purpose, the geometric modeler should be embedded into the design procedure which is composed of the grid generation tool, the Computation Fluid Dynamics (CFD) solver and the optimization tool.

In the framework of the national project BULBE , we intend to use the commercial software package FINE/Marine from NUMECA, that gathers the grid generation software Hexpress and the solver Isis-CFD, in collaboration with K-Epsilon company.

The geometrical model, based on the methods presented above, has been implemented in the AXEL Platform developed by INRIA Galaad Project-Team. To export the resulting geometry to the grid generation tool, some additional steps have been introduced: firstly, the hull surface is embedded into a closed box used to define the computational domain. Secondly, all the surfaces are triangulated to obtain a discrete description of the domain boundary, written in an input file for the grid generation tool. Figure 7 illustrates these two steps necessary for exporting the geometrical model. We refer to [3] (C annex) for details concerning the description of the file.

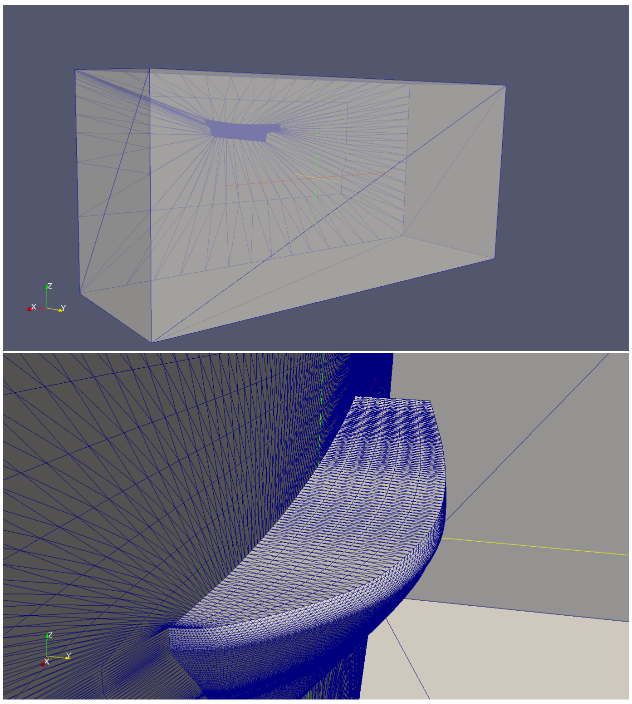

Figure 7: Domain description for computation (the shape of the trawler ship and the box) .

Conclusion

Two approaches have been developed and tested to generate automatically bow shapes for a trawler ship.

The first one, based on fitting methods with regularization, seems to be promising because it allows to use very detailed shape targets. However, this approach still requires to mature for industrial use. In particular, one should improve the constraints applied on the shape in order to avoid unrealistic oscillations.

The second one, based on a direct handling of meta-parameters, is far easier to use but is more limited in terms of shape definition.

Acknowlegement

This work is funded by the Ministry of Fishing DPMA (Direction des Pêches Maritimes et de l'Aquaculture) and the European Fund for Fishing. It gathers INRIA OPALE Project-Team, K-Epsilon company (specialized in CFD for naval hydrodynamics, see `http://www.k-epsilon.com`) and PROFIL company (naval architect, see `http://www.jean-et-frasca.com`). The objective is to design and optimize bow shapes for trawler ships, in order to reduce the fuel consumption during fishing campaigns.

References

[1] Xiao-Diao Chen, Gang Xu, Jun-Hai Yong, Guozhao Wang, and Jean-Claude Paul. Computing the minimum distance between a point and a clamped B-spline surface. *Graphical Models*, 71(3):107–112, April 2009.

[2] Philip E. Gill, Walter Murray, and Margaret H. Wright. *Practical optimization*. Academic Press Inc. [Harcourt Brace Jovanovich Publishers], London, 1981.

[3] Pierre-Luc Perrier. Module de maillage parametrique pour la cfd. *Stage de fin d'etude.*, 2011.

[4] Helmut Pottmann, Stefan Leopoldseder, and Michael Hofer. Approximation with active b-spline curves and surfaces. pages 8–25, 2002.

[5] Jules Proust. Modelisation et optimisation de carenes. *Stage de fin d'etude.*, 2011.

[6] Wenping Wang, Helmut Pottmann, and Yang Liu. Fitting b-spline curves to point clouds by squared distance minimization. *ACM TRANSACTIONS ON GRAPHICS*, 25, 2004.

Contents

RESEARCH CENTRE
SOPHIA ANTIPOLIS – MÉDITERRANÉE

2004 route des Lucioles - BP 93
06902 Sophia Antipolis Cedex

Publisher
Inria
Domaine de Voluceau - Rocquencourt
BP 105 - 78153 Le Chesnay Cedex
inria.fr

ISSN 0249-6399